Kinetic modelling of the nitric oxide gradient generated *in vitro* by adherent cells expressing inducible nitric oxide synthase

Michel LAURENT*‡, Michel LEPOIVRE† and Jean-Pierre TENU†

*Service d'Imagerie Cellulaire, URA 1116, Bâtiment 441, Université Paris-Sud, Centre d'Orsay, 91405 Orsay Cedex, France,
and †Laboratoire des Immunomodulateurs d'Origine Bactérienne, URA 1116, Bâtiment 432, Université Paris-Sud, Centre d'Orsay, 91405 Orsay Cedex, France

Inducible nitric oxide (NO) synthase produces a long-lasting NO flux which can exert cytotoxic effects on target cells. A prerequisite for the understanding of the molecular basis of NO action is quantitative data on the availability of this small neutral radical molecule at both the spatial and temporal levels. The limits of NO availability depend on the respective rates of NO production, diffusion and autoxidation by molecular oxygen. Kinetic modelling of these processes has been performed for a widely used experimental system consisting of a monolayer of adherent cells cultured *in vitro* for hours in unstirred culture medium. It appears that: (i) the maximal NO concentration in the culture is in the immediate vicinity of the monolayer, where target cells will sediment; (ii) the steady-state NO concentration in this area is lower than 4 to 5 μM; and (iii) measurements of nitrite/nitrate or citrulline accumulation in the bulk cell medium culture during a given time period significantly underestimate (by a factor of up to 3 to 4) the true rate of NO synthesis at the level of the producer cell. This rate can be, nevertheless, easily estimated from the rate of production of the stable NO synthase products.

INTRODUCTION

Nitric oxide (NO) is a small radical molecule which can diffuse readily across biological membranes to reach intracellular targets [1]. NO thus behaves as a messenger in cell-to-cell interactions but is also potentially cytotoxic, depending on its concentration and on the redox status of its environment. In mammalian cells, several NADPH-dependent flavoproteins, named nitric oxide synthases (NOSs), are responsible for the biosynthesis of NO by oxidation of the guanido group of L-arginine [2]. Citrulline and NO_2^-/NO_3^- are the final, stable products of the reaction.

NOSs are either constitutive or inducible enzymes. The constitutive NOS isoforms (also known as types I and III) are rapidly activated by the calcium/calmodulin complex upon appropriate agonist stimulation in intact cells, whereas inducible NOSs (type II) are calcium-insensitive. The constitutive enzymes produce short-lasting and small quantities of NO, which acts, for instance, as an endothelium-derived relaxing factor [3], regulates platelet aggregation [4] and behaves as a neuromediator [5]. The calcium-insensitive enzyme can be induced in many cell types by immunomodulators such as cytokines (interferon-γ, tumour necrosis factor α, interleukin-1) and bacteria-derived molecules (lipopolysaccharide, muramyldipeptide) [6]. Larger quantities of NO are produced over a longer period (up to several days) by the inducible NOS isoform. NO produced in this way is the main effector molecule responsible for the anti-proliferative effect exerted by activated rodent macrophages: NO has a physiopathological role as an anti-viral, anti-bacterial, anti-parasite and anti-tumour agent [5].

In order to understand the physiological reactivity of NO, true NO concentrations have to be quantified in various experimental situations. Spectrophotometric or electrochemical measurements of NO produced for a short time by constitutive NOSs have been already made with this aim (reviewed in ref. [7]). However, only a few attempts have been reported for direct measurement of long-lasting NO production by cell cultures containing induced NOSs (this has been done essentially by using chemiluminescence [8,9] and spin-trapping methods [10,11]). In most cases, data are expressed as end-product (nitrite, nitrate, citrulline) accumulation during a given time interval, but the real steady-state concentration of NO in the culture medium remains unknown. As another approach for estimating NO concentrations, models of the diffusional spread of NO have previously been proposed to account for endothelial [12] and neuronal [13] NO signalling. However, these two models did not take into account oxidation of NO by dissolved molecular oxygen (autoxidation). Such a simplification is probably justified when short NO pulses are produced by constitutive NOSs. However, it no longer holds when NO is synthesized continuously for hours by inducible NOSs since, under these conditions, autoxidation becomes the main NO-consuming process responsible for nitrite accumulation. In this paper, we present new calculations which take into account both the diffusion of NO into the culture medium [1,12] and the kinetics of its autoxidation in aqueous solutions [14]. We show that, under widely used *in vitro* experimental conditions, the various effects of NO on target cells are expected to occur in a concentration range lower than 4–5 μM. In addition, we have found that, although the NO distribution in the culture medium is generally far from homogeneous, the average rate of nitrite or citrulline synthesis measured in the bulk cell culture medium can be used to calculate the NO concentration in the immediate vicinity of the effector cells.

METHODS AND RESULTS

Description of the model

Adherent cells activated for inducible NOS expression were supposed to be lying at the bottom of a Petri dish or a microtest well. After washing, fresh medium containing L-arginine was assumed to be poured over the cell layer, which then begins producing NO for hours. This situation is typical of experimental measurements of NO released from adherent effector cells like macrophages, after a preculture phase for NOS induction.

Abbreviations used: NO, nitric oxide; NOS, nitric oxide synthase.

‡ To whom correspondence should be addressed.

Kinetic simulations were carried out using the following assumptions.

(1) NO is released from adherent cells at a constant rate v. The height (x) axis is such that cells are found at $x = 0$ and the interface air/medium at $x = x_0$.

(2) The system is either closed for NO (its finite length corresponds to the height x_0 of the aqueous phase) or a depletion of NO may arise at distance x_0. This latter hypothesis simulates the case in which NO disappears at the interface between the gas phase and the aqueous phase. A rapid evaporation of dissolved NO is likely, because of an air:water partition coefficient of about 20:1 [7].

(3) Diffusion of NO in the medium is described by Fick's second law: diffusion is proportional to the second spatial derivative $\partial^2[NO]_{x,t}/\partial x^2$.

(4) In aqueous, aerobic solution, diffusion of NO is hindered by chemical reaction, i.e. NO autoxidizes to NO_2^-. According to Kharitonov et al. [14], autoxidation of NO has a second-order concentration dependence on NO and a first-order concentration dependence on O_2:

$$d[NO_2^-]/dt = k_3[O_2][NO]^2$$

In experimental systems, the aqueous medium is in equilibrium with the air phase. Thus, the slight O_2 consumption by cell respiration is balanced by O_2 redissolving from the air phase. Moreover, the rate of NO production is very low compared with the estimated concentration of O_2 in aqueous phase, preventing the possible formation of a gradient of O_2. Hence, the O_2 concentration may be assumed to be constant and we can define k: $k = k_3[O_2]$.

Patterns of spatiotemporal distribution of NO

According to these assumptions, the concentration of NO in the aqueous phase, at time t and at distance x from the point source, is given by the solution of the following partial differential equation:

$$\partial[NO]_{x,t}/\partial t = v - k[NO]_{x,t}{}^2 - D(\partial^2[NO]_{x,t}/\partial x^2) \quad (1)$$

where D is the diffusion coefficient for NO. Taking into account the geometry of the system, diffusion along a single dimension x has to be considered. Eqn. (1) may be solved numerically with specific values for the constants v, k and D obtained as far as possible from experimental data. In our simulations, we chose the following values: $1.7 \times 10^{-8} > v > 1 \times 10^{-10}$ $M \cdot s^{-1}$ at $x = 0$ and $v = 0$ at $x \neq 0$; $k = 10^3$ $M^{-1} \cdot s^{-1}$ and $D = 3 \times 10^{-5}$ $cm^2 \cdot s^{-1}$ [12].

The depth x_0 of the aqueous phase was either 3 or 6 mm. The value of the pseudo-second-order rate constant k agrees with the value of k_3 (6×10^6 $M^{-2} \cdot s^{-1}$) determined by Kharitonov et al. [14] and the previously estimated concentration of molecular O_2 in aqueous phase (0.22×10^{-3}M) [15].

Considering the space as a linear mesh of equidistant points, diffusion terms were represented in the form of central finite differences. The resulting ordinary differential equation was integrated, in each compartment, by means of a Runge-Kutta method. We verified that use of a 5-fold smaller distance increment does not change the results of integration.

Rate of NO production at the level of the cell layer

At the level of the cell monolayer producing NO ($x = 0$), the limiting value in the absence of a significant rate of loss from the cells by diffusion is:

$$d[NO]_{x=0,t}/dt = v - k[NO]^2{}_{x=0,t} \quad (2)$$

Taking into account initial conditions ($[NO]_{x=0,t} = 0$ when $t = 0$), eqn. (2) becomes an ordinary differential equation which may be solved as:

$$t = \frac{1}{2\sqrt{(kv)}} \ln \left[\frac{\sqrt{\frac{v}{k}} + [NO]_{z=0}}{\sqrt{\frac{v}{k}} - [NO]_{z=0}} \right] \quad (3)$$

The half-time of the reaction ($t_{\frac{1}{2}}$) is given by:

$$t_{\frac{1}{2}} = \ln 3/[2\sqrt{(kv)}]$$

and the asymptotic steady-state concentration of NO at the surface of the cell layer ($[NO]_{SS,x=0}$) is:

$$[NO]_{SS,x=0} = \sqrt{(v/k)}$$

Mean rate of nitrite formation in the aqueous phase

Usually, the concentration of NO is estimated from the concentration of nitrite, a product of NO autoxidation easily measured by the Griess assay [16]. Of course, the latter is not measured at every distance from the cells producing NO but a mean value ($[NO_2^-]_t$ at time t) in the total aqueous phase is determined. With the previous assumptions and knowing the spatiotemporal distribution of NO, the mean rate (v_{mean}) of nitrite production in aqueous phase may be calculated as follows:

$$v_{mean} = \frac{\overline{[NO_2^-]_t}}{t} = \frac{\int_0^{x_0} k[NO]^2{}_x \, dx}{x_0} = \frac{\sum_{x=0}^{n} k[NO]^2{}_x}{n+1}$$

$$= k[NO]^2{}_{x=0} \left[\frac{\sum_{x=0}^{n} \left(\frac{[NO]_x}{[NO]_{x=0}} \right)^2}{n+1} \right] \quad (4)$$

where n is the number of compartments used in the calculations ($n = 30$ or 60 in our simulations with a mesh size of 100 μm). It is important to emphasize that v_{mean} corresponds to the experimental parameter used to estimate the mean rate of nitrite formation and that eqn. (4) only formalizes the empirical procedure consisting of the measurement of the total amount of NO_2^-, which is then divided by the volume of the aqueous phase and by the time period of production.

Numerical results

Spatiotemporal distributions of NO are shown in Figure 1, in the case of a system with a finite length which corresponds to the height x_0 of the culture medium above the cell layer. This is the case, for example, for a Petri dish of 35 mm diam. containing 2.5 ml of medium ($x_0 = 3$ mm, Figure 1A) or a microtest culture well containing 0.2 ml of medium ($x_0 = 6$ mm, Figure 1B). In both cases, spatial distributions of NO reach non-homogeneous steady states after between a few minutes and tens of minutes, depending on the rate v of NO production.

When the constant flux v of NO synthesis by the cell layer is two orders of magnitude lower than in the case of Figure 1(A), the spatial distribution of NO becomes nearly homogeneous at steady state (Figure 1C); however, the stationary-state value for NO is reached much more slowly. For instance, in the conditions depicted under Figure 1(C), the half-time is 29 min in compartment 1, at the level of the cell layer (Figure 1C).

In the previous simulations, no depletion of NO was supposed to occur at the interface between the air phase and the aqueous

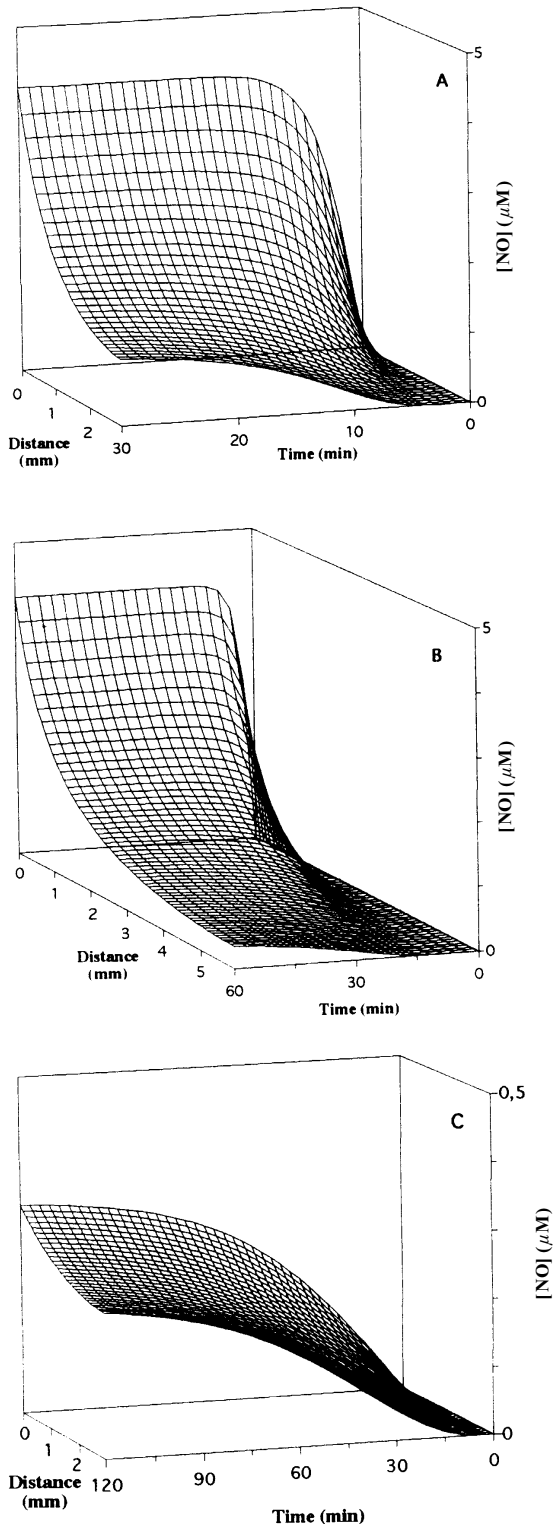

Figure 1 Spatiotemporal distribution, in the aqueous phase, of NO released from adherent cells lying at the bottom of a Petri dish (A and C) or a microtest well (B)

Cell layer position was defined as the origin of the distance axis ($x = 0$). Data were calculated by numerical integration of eqn. (1) using the following set of parameters: $D = 3 \times 10^{-5}$ cm$^2 \cdot$s^{-1}, $k = 10^3$ M$^{-1} \cdot$s^{-1} and $v = 1.7 \times 10^{-8}$ M$\cdot$s^{-1} (**A** and **B**) or 10^{-10} M$\cdot$s^{-1} (**C**). In (**A**) and (**C**), the total height of the aqueous phase is 3 mm, whereas it is 6 mm in the case of (**B**). No depletion of NO was supposed to occur at the interface between the air phase and the aqueous phase.

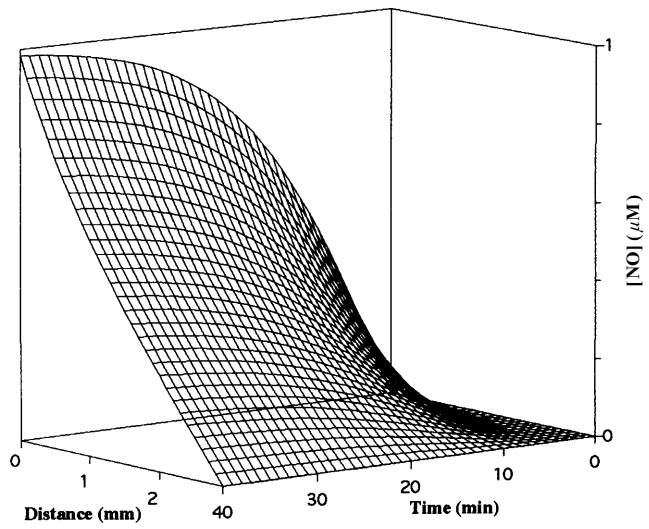

Figure 2 Effect of a total depletion of NO occurring at the air/medium interface on the gradient of NO concentration observed along the distance axis

Data were calculated by numerical integration of eqn. (1) using the following set of parameters: $D = 3 \times 10^{-5}$ cm$^2 \cdot$s^{-1}, $k = 10^3$ M$^{-1} \cdot$s^{-1} and $v = 10^{-9}$ M$\cdot$s^{-1}. To simulate the total depletion of NO at the air/medium interface, boundary conditions were chosen so that the NO concentration in the last compartment (at $x = 3$ mm) was held at 0 for each time-point.

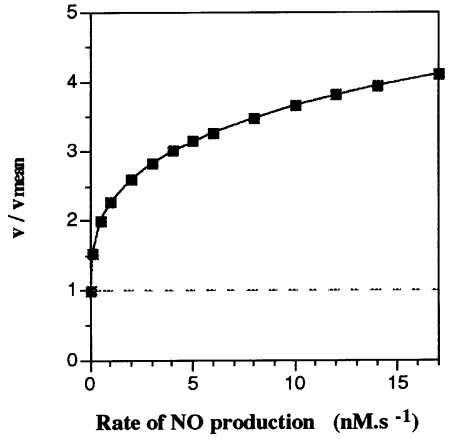

Figure 3 Comparison of the true rate (v) of NO released at the level of the cell layer with the mean rate (v_{mean}) of NO_2^- production measured experimentally in the bulk aqueous medium (with a 3 mm height), for different values of v

In these calculations, depletion of NO at the air/medium interface was neglected. Each point was calculated using eqn. (2) for v and eqn. (4) for v_{mean}. In both cases, v and v_{mean} rates correspond to steady-state values. The values for the $[NO]_x$ variable in eqn. (4) were determined by numerical integrations of eqn. (1) (with $D = 3 \times 10^{-5}$ cm$^2 \cdot$s^{-1} and $k = 10^3$ M$^{-1} \cdot$s^{-1}) which were carried out until the steady state was reached.

phase. If we now suppose that a fast total escape occurs at the air/medium interface, the gradient of NO concentration observed at steady state along the distance axis tends to be linear. This is illustrated in Figure 2, for a value of v equal to 1 nM$\cdot$s^{-1} and a liquid height of 3 mm. In a more realistic case in which removal to air is proportional to the NO concentration in the compartment

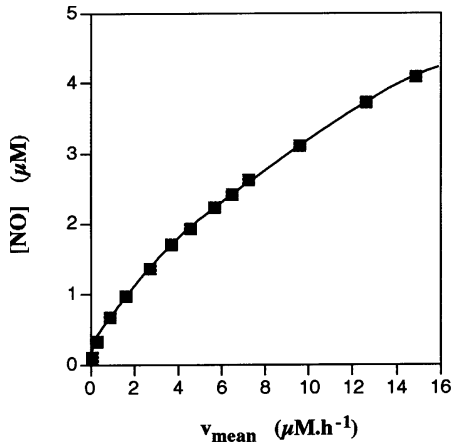

Figure 4 Steady-state concentrations of NO close to the cell monolayer, as a function of v_{mean}

The rate v of NO released at the level of the cell layer ($x = 0$) was calculated from v_{mean} (mean rate of nitrite production), as described in Figure 3. The steady-state NO concentration at $x = 0$ was calculated with this value by integration of eqn. (1) ($D = 3 \times 10^{-5}$ cm$^2 \cdot$s^{-1} and $k = 10^3$ M$^{-1} \cdot$s^{-1}, no depletion of NO at the air/medium interface).

at the interface, the gradient of NO would have an intermediary shape between those of Figures 1 and 2.

Whatever the form of the distribution gradient of NO along the distance axis, the stationary rate of NO_2^- production at the level of the cell layer ($k[NO]^2_{x=0}$) approaches a limiting value equal to the rate v of NO synthesis by cells. In the absence of any loss to air, this may be seen as a consequence of mass conservation in a closed system. This value v is significantly larger than the average rate v_{mean} of NO_2^- production (eqn. 4) which can be measured in the bulk medium (Figure 3). The larger the rate v, the greater the difference between v and v_{mean}. It is noteworthy that the true rate v of NO synthesis and the steady-state NO concentration in the close vicinity of the cells can be estimated from the experimental average rate v_{mean} of NO_2^- production (Figures 3 and 4, respectively).

DISCUSSION

In this paper, we present a new model that describes the spatiotemporal distribution of NO concentrations produced by a long-lasting inducible NOS activity expressed *in vitro* in adherent cell culture. This model is the first one to take into account both the diffusion of NO and its autoxidation by O_2. We show that a monolayer of adherent cells progressively generates a gradient of NO concentration that stabilizes under steady-state conditions and is determined by the rate v of NO production, the height of the culture medium above the monolayer and the O_2 concentration. The steepness and the shape of the gradient depend on the volume of the culture, which is a parameter that does not influence the maximal concentration of NO found at the level of the cell layer. Interestingly, this maximum can be derived from the direct easy measurement, in the bulk medium, of the average rate of NO_2^- production. Although nitrite is the only oxidation product of NO produced from purified NOS, this is not the case in complex cell cultures, where NO is also partially transformed into NO_3^-. Thus, an accurate estimation of the mean rate of NO production requires the measurement of NO_2^- and NO_3^-, or citrulline if not recycled through the urea metabolic cycle. Hence, citrulline produced by murine peritoneal macrophages appears to be a relevant parameter [17]. Our earlier experiments [18], using a high density of activated murine macrophages producing NO (4×10^6 macrophages in 2.5 ml in a Petri dish of 33 mm diam.), indicated a maximal value of citrulline accumulation of around 160 μM after 10 h, which corresponds to a mean rate v_{mean} of about 16 μM$\cdot$h^{-1}. This probably represents one of the highest obtainable values since we could not find a higher one in the literature [19–22]. From these results, a value for the v parameter [in eqn. (4) and in Figure 3] close to 60 μM$\cdot$h^{-1} (i.e. 17 nM$\cdot$s^{-1}) seems to be a reasonable maximum, which leads to the determination of a maximal steady-state NO concentration of about 4 μM in the immediate vicinity of the producing cells. Under these conditions, the half-time of the process is 2.2 min and 95 % of the steady-state value is reached within 7 min. Even if the rate of production v were increased to 25 nM$\cdot$s^{-1}, the NO concentration at steady state in the immediate vicinity of the macrophages would only reach 5 μM (with a half-time of 1.8 min, so that 95 % of the steady-state value of NO concentration would be obtained within 6 min). If v were lower (varying from 0.1 to 1 nM$\cdot$s^{-1} for instance, by changing the macrophage density), the autoxidation process would become very slow (half-times of about 30 and 9 min respectively), the stationary-state concentration of NO in the vicinity of the producing cells being approx. 0.3 to 1 μM. Under the former conditions ($v = 0.1$ nM$\cdot$s^{-1}), the mean rate of nitrite production in the aqueous phase is no longer significantly different from the true rate of NO production and, in the absence of NO evaporation, the distribution of NO in the medium is homogeneous.

We are aware that our data might be overestimates if NO is consumed in pathways other than autoxidation, such as reactions with $O_2^{\cdot-}$, other radicals or transition metals [23]. The predicted maximum of 4–5 μM of NO close to the effector cell layer is therefore a real limit. This value is consistent with a free NO concentration of 0.32 μM generated by lipopolysaccharide-activated rat alveolar macrophages and measured by an NO-sensitive electrode [24]. In contrast, the steady-state NO concentration in human monocyte cultures is certainly lower: a 0.1–0.2 μM concentration range of NO at steady state can be calculated from the reported 10–40 μM of nitrite accumulated over 8 days in culture medium [25].

From a practical point of view, we can assume that when target cells (i.e. tumour cells) are introduced into fresh medium over a washed layer of effector cells (such as murine macrophages) in which the NOS enzyme has been induced, a steady-state concentration of NO is reached in a time-scale ranging from a few minutes to tens of minutes. During this time, target cells are allowed to sediment close to the effector cell layer, so that they become surrounded by an effective NO concentration which cannot exceed 4–5 μM. As a consequence, putative explanations of the *in vitro* cytostatic effects of NO on target cells, such as inhibition of iron-containing enzymes (complexes I and II of the respiratory chain, aconitase [26–28] or ribonucleotide reductase [29]), have to be consistent with a sustained NO concentration in the micromolar range. This also has to be true for other molecular targets of inducible NOS action [23]. In this field, it was shown recently that NO, at concentrations below 1 μM, can reversibly inhibit respiration by competing with oxygen at cytochrome oxidase [30]. Finally, it should be noted that concentrations of NO produced by constitutive NOSs in cell monolayers are in the same order of magnitude as the steady-state NO levels generated by inducible NOSs, according to our model (100–1300 nM of NO measured by NO-electrodes [31,32] versus calculated concentrations of 100–4000 nM respectively). Therefore, we would like to propose that the major difference between constitutive and inducible NOS activities does not reside in the concentration of

NO that they generate in the vicinity of the effector cell, but rather depends on the period of time (i.e. minutes versus days) during which they are able to produce NO.

This work was supported by grants from the CNRS, the Université Paris-Sud and the Ligue Nationale contre le Cancer. We thank Dr. Gillian Barratt for careful reading of the manuscript.

REFERENCES

1 Vanderkooi, J. M., Wright, W. W. and Erecinsha, M. (1994) Biochim. Biophys. Acta **1207**, 249–259
2 Nathan, D. (1992) FASEB J. **6**, 3051–3064
3 Palmer, R. M. J., Ferridge, A. G. and Moncada, S. (1987) Nature (London) **327**, 524–526
4 Radomski, M. W., Palmer, R. M. J. and Moncada, S. (1990) Proc. Natl. Acad. Sci. U.S.A. **87**, 5193–5197
5 Snyder, S. H. (1992) Curr. Neurobiol. **2**, 323–327
6 Nussler, A. K. and Billiar, T. R. (1993) J. Leukocyte Biol. **54**, 171–178
7 Archer, S. (1993) FASEB J. **7**, 349–360
8 Hibbs, J. B., Taintor, R. R., Vavrin, Z. and Radilin, E. M. (1988) Biochem. Biophys. Res. Commun. **157**, 87–94 (Erratum published in Biochem. Biophys. Res. Commun. **158**, 624)
9 Sung, Y. J., Hotchkiss, J. H., Austic, R. E. and Dietert, R. R. (1992) Biochem. Biophys. Res. Commun. **184**, 36–42
10 Lancaster, J. R. and Hibbs, J. B. (1990) Proc. Natl. Acad. Sci. U.S.A. **87**, 1223–1227
11 Vanin, A. F., Mordvintcev, P. I., Hauschildt, S. and Mülsch, A. (1993) Biochim. Biophys. Acta **1177**, 37–42
12 Lancaster, J. R. (1994) Proc. Natl. Acad. Sci. U.S.A. **91**, 8137–8141
13 Wood, J. and Garthwaite, J. (1994) Neuropharmacology **33**, 1235–1244
14 Kharitonov, V. G., Sundquist, A. R. and Sharma, V. S. (1994) J. Biol. Chem. **269**, 5881–5883
15 Wink, D. A., Darbyshire, J. F., Nims, R. W., Saavedra, J. E. and Ford, P. C. (1993) Chem. Res. Toxicol. **6**, 23–27
16 Green, L. C., Wagner, D. A., Glogowski, J., Skipper, P. L., Wishnok, J. S. and Tannenbaum, S. R. (1982) Anal. Biochem. **126**, 131–138
17 Chénais, B., Yapo, A., Lepoivre, M. and Tenu, J. P. (1991) J. Chromatogr. **539**, 433–441
18 Chénais, B. (1994) Ph.D. Thesis, University of Paris XI, France
19 Stuehr, D. J. and Marletta, M. A. (1987) J. Immunol. **139**, 518–525
20 Drapier, J. C., Wietzerbin, J. and Hibbs, J. B. (1988) Eur. J. Immunol. **18**, 1587–1592
21 Green, S. J., Chen, T. Y., Crawford, R. M., Nacy, C. A., Morrison, D. C. and Meltzer, M. S. (1992) J. Immunol. **149**, 2069–2075
22 Jun, C. D., Choi, B. M., Ryu, H., Um, J. Y., Kwak, H. J., Lee, B. S., Paik, S. G., Kim, H. M. and Chung, H. T. (1994) J. Immunol. **153**, 3684–3690
23 Stamler, J. S. (1994) Cell **78**, 931–936
24 Greenberg, S. J., Xie, J. M., Wang, Y., Kolls, J., Malinski, T., Summer, W. R. and Nelson, S. (1994) Alcohol **11**, 539–547
25 Mautino, G., Paul-Eugène, N., Chanez, P., Vignola, A. M., Kolb, J.-P., Bousquet, J. and Dugas, B. (1994) J. Leukocyte Biol. **56**, 15–20
26 Drapier, J. C. and Hibbs, J. B. (1988) J. Immunol. **140**, 2829–2838
27 Hansladen, A. and Fridovich, I. (1994) J. Biol. Chem. **269**, 29405–29408
28 Castro, L., Rodriguez, M. and Radi, R. (1994) J. Biol. Chem. **269**, 29409–29415
29 Lepoivre, M., Chénais, B., Yapo, A., Lemaire, G., Thelander, L. and Tenu, J. P. (1990) J. Biol. Chem. **265**, 14143–14149
30 Brown, G. C. and Cooper, C. E. (1994) FEBS Lett. **356**, 295–298
31 Malinski, T., Taha, Z., Grunfeld, S., Patton, S., Kapturczak, M. and Tombolian, P. (1993) Biochem. Biophys. Res. Commun. **193**, 1076–1082
32 Tsukahara, H., Gordienko, D. V. and Goligorsky, M. S. (1993) Biochem. Biophys. Res. Commun. **193**, 722–729

Received 24 July 1995/27 September 1995; accepted 10 October 1995